Organic & Biomolecular Chemistry



PAPER

View Article Online
View Journal | View Issue



Cite this: *Org. Biomol. Chem.*, 2024, **22**, 5224

Received 8th April 2024, Accepted 1st June 2024 DOI: 10.1039/d4ob00573b

rsc.li/obc

Chemodivergent phosphonylation of diazocarboxylates: light-on vs. light-off reactions†

Jalaj Kumar Pathak, a,b Ruchir Kant^c and Namrata Rastogi 🕞 *a,b

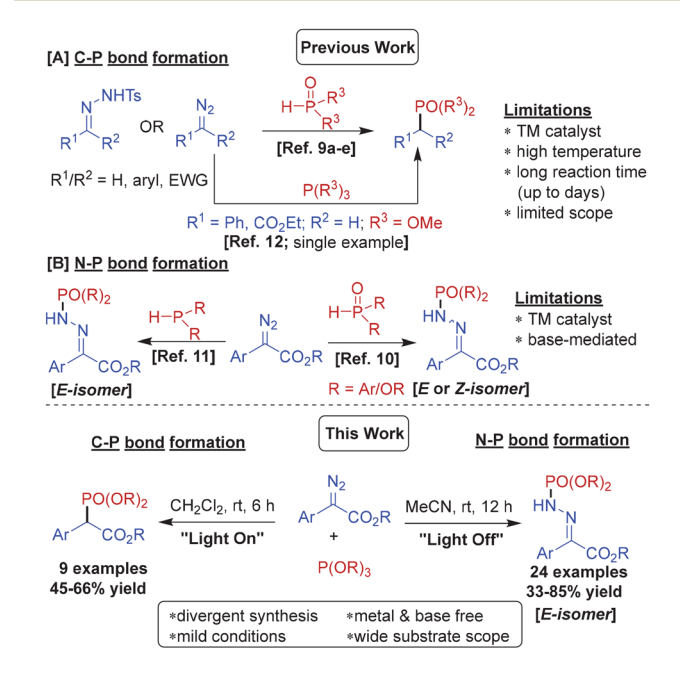
By tapping into the divergent reactivity of diazocarboxylates under thermal and photocatalytic conditions, we could develop chemodivergent phosphonylation protocols for α -diazocarboxylates with trialkyl phosphites. While the thermal reaction led to N-P bond formation affording phosphonylated hydrazones, the visible light-mediated reaction furnished phosphonylated aryl carboxylates through C-P bond formation. Both reactions are notable for their operational simplicity and mild conditions affording products in good yields without the requirement of a metal, base or photocatalyst.

Introduction

Phosphorus containing organic scaffolds are found extensively among natural as well as synthetic medicinal compounds, agrochemicals and functional materials. Organophosphorus compounds are also valuable as catalysts, ligands, protecting groups and building blocks in organic chemistry. Therefore, numerous synthetic methods to incorporate phosphorus into organic scaffolds have been invented. Yet development of more efficient protocols to access various organophosphorus molecules is highly desired.

The diazo compounds are undoubtedly amongst the most versatile organic substrates owing to their tendency to serve as dipoles, nucleophiles, electrophiles, and precursors to carbenes, ketenes and radical intermediates. This unique reactivity profile of the diazo group offers great opportunity to develop chemodivergent reactions by modulating the reaction conditions. For instance, aryl diazoacetates form free carbenes upon visible light irradiation whereas they serve as C-nucleophiles and N-electrophiles under thermal conditions. We envisioned that a nucleophile would undergo both an insertion reaction with the electrophilic diazocarbene and nucleophilic addition reaction with the terminal nitrogen of the diazo group, under suitable conditions. We opted to explore the phosphorus nucleophiles for these reactions con-

sidering the significance of organophosphorus scaffolds, as mentioned above, and also because phosphorus can adopt various oxidation states offering options for further transformation of the products. Notably, several reactions of diazo compounds with P(O)H compounds to access organophosphorus scaffolds featuring C-P or N-P linkages have been reported in the recent literature. For instance, phosphine oxides undergo transition metal-mediated P-H insertion or reductive catalytic coupling with diazo substrates (or diazo intermediates *in situ* generated from tosylhydrazones) forming C(sp³)-P bonds (Scheme 1A). On the other hand, Zhu and co-workers reported



Scheme 1 Carbon vs. nitrogen phosphonylation of diazo compounds.

^aMedicinal & Process Chemistry Division, CSIR-Central Drug Research Institute, Lucknow-226031, India. E-mail: namrata.rastogi@cdri.res.in

^bAcademy of Scientific and Innovative Research (AcSIR), Ghaziabad-201002, India ^cBiochemistry & Structural Biology Division, CSIR-Central Drug Research Institute, Lucknow-226031. India

[†]Electronic supplementary information (ESI) available: ¹H, ¹³C, ³¹P and ¹⁹F NMR spectra of all new compounds. CCDC 2342436. For ESI and crystallographic data in CIF or other electronic format see DOI: https://doi.org/10.1039/d4ob00573b

a base-mediated nucleophilic addition of phosphonates with α -diazoesters resulting in *E*-phosphinamides with N–P bonds (Scheme 1B). However, during the preparation of this manuscript Nan and Yi published photocatalytic phosphonylation of H-phosphine oxides with α -diazoesters to afford *Z*-phosphinic hydrazones. Similar N–P bond formation was reported by Pullarkat and Leung through palladium-catalyzed asymmetric diarylphosphine addition to α -diazoesters leading to the enantioenriched phosphinic hydrazones (Scheme 1B).

To the best of our knowledge phosphites have never been used as substrates with diazo compounds except for an iron-catalyzed reaction of trimethyl phosphite with phenyldiazomethane and ethyl diazoacetate forming dimethyl benzylphosphonate and ethyl 2-(dimethoxyphosphoryl)acetate, respectively, through a phosphorus ylide intermediate¹² (Scheme 1A). We hereby report diazocarboxylate phosphonylation with phosphites *via* nucleophilic substitution or carbene insertion generating divergent organophosphorus scaffolds featuring N–P or C–P bonds, respectively, by simple "switch-off" or "switch-on" of blue light (Scheme 1; this work).

We first started investigating the nucleophilic substitution reaction with methyl 2-diazo-2-phenylacetate **1a** and trimethyl phosphite **2a** as model substrates (Table 1).

The initial experiments with 1a and 2a in a 1:1 ratio employing DMSO or DMF as the solvent at room temperature failed to furnish any identifiable product (entries 1 and 2). Upon changing the solvent to toluene, the expected phosphinamide product 3a was isolated in 15% yield (entry 3). Further solvent screening revealed moderate and almost similar yields in methanol (40%) and dichloromethane (42%) (entries 4 and 5). However, the yield improved to 50% in acetonitrile with comparable yields in chloroform (48%) and acetone (46%)

Table 1 Optimization of conditions for thermal phosphonylation^{a,b}

		PO(OMe) ₂
N_2	P(OMe) ₃	HŇ. _N
↓	2a	
Ph CO ₂ Me 1a	Solvent, rt	Ph CO ₂ Me 3a

Entry	1a:2a	Solvent	Yield of $3a^c$ (%)
1^d	1:1	DMSO	0
2^d	1:1	DMF	0
3	1:1	PhMe	15
4	1:1	MeOH	40
5	1:1	CH_2Cl_2	42
6	1:1	$CHCl_3$	48
7	1:1	$(Me)_2CO$	46
8	1:1	MeCN	50
9	2:1	MeCN	45
10	1:2	MeCN	66
11	1:3	MeCN	78
12	1:4	MeCN	72
13 ^e	1:3	MeCN	75

^a Unless otherwise mentioned, the reactions were carried out on a 0.2 mmol scale of **1a** with specified amounts of **2a** in 2 mL solvent at rt under N₂. ^b Time taken for reaction completion: 10–12 h. ^c Isolated yields. ^d Complex mixture. ^e Reaction in 1 mL solvent.

(entries 6–8). Further, the reaction with a 2:1 substrate ratio of 1a and 2a furnished 3a in 45% yield (entry 9) but reversing the ratio to 1:2 led to the isolation of 3a in 66% yield (entry 10). Further optimization of the reaction conditions established that a 1:3 ratio of 1a and 2a in acetonitrile were the best conditions affording 3a in 78% isolated yield (entries 8–12). Apparently, the yields were largely independent of the reaction concentration since 3a was isolated in 75% yield in a more concentrated mixture of 1a and 2a taken in a 1:3 ratio (entry 13). The product was isolated as exclusively the *E*-isomer, as identified by ¹H NMR and single crystal X-ray analysis of 3k. ¹³

After optimizing the reaction conditions, we set out to determine the scope of the thermal phosphonylation reaction. For this purpose, several α-diazo esters **1a–1q** and trialkylphosphites **2a–2d** were subjected to the optimized reaction conditions (Table 2). Initially, trimethyl phosphite **2a** was used as the reaction partner with various electron-rich and electron-deficient aryl diazocarboxylates to afford the corresponding phosphinamides **3a–3l** in high yields ranging from 33–85%. Notably, commonly encountered functional groups such as –OMe, –OCF₃, –Ph, –CF₃, –NO₂ and halogens (Cl, Br, F) on the aryl ring of the diazo substrate were tolerated well in the reaction. The reaction of trimethyl phosphite **2a** also proceeded smoothly with methyl 2-diazo-2-(naphthalen-1-yl)acetate and heteroaryl substrates such as ethyl 2-(benzo[d][1,3]dioxol-5-yl)-2-diazoacetate and ethyl 2-diazo-2-(thiophen-3-yl)acetate to

Table 2 Scope of thermal phosphonylation of diazo compounds a,b

^a Reaction conditions: 1 (0.2 mmol) and 2 (0.6 mmol) in CH₃CN (2 mL) at rt under N₂. ^b Isolated yields mentioned. ^c Isolated yield for a 5 mmol scale reaction.

3w. 56%

3v, 65%

3u, 70%

3x. 80%

furnish the corresponding products 3m, 3n and 3o in high yields. Moreover, a phenyldiazoester with an allyl acetate group 1p and a propargyl acetate group 1q also reacted well with 2a to yield 3p and 3q in 63 and 60% yields, respectively. Further, the N-phosphonylation of aryldiazocarboxylate 1a could also be carried out efficiently with other trialkyl phosphites such as triethyl phosphite 2b, triisopropyl phosphite 2c and triallyl phosphite 2d to afford 3r-3t in 65-72% yields.

Eventually, the N-phosphonylation reaction could be successfully extended to other diazo substrates bearing at least one acceptor group including 2-diazo-1,2-diphenylethan-1-one (1r), (1-diazo-2,2,2-trifluoroethyl)benzene (1s), diethyl 2-diazomalonate (1t) and 2-diazo-1,3-diphenylpropane-1,3-dione (1u) furnishing the corresponding products 3u-3x in excellent vields.

The E-configuration was assigned to the products on the basis of analogy with 3k, the structure of which was confirmed by single X-ray crystallography (Fig. 1).13

Next, we set out to establish the suitable conditions for the proposed photochemical phosphonylation reaction between 1a and 2a (Table 3).

To begin with, equivalent amounts of 1a and 2a were reacted in various solvents under blue light irradiation. The reactions in both dimethyl sulfoxide and dimethyl formamide were too complex to be conclusive (entries 1 and 2). In toluene, although the reaction furnished the anticipated C-P phosphonylation product 4a in 15% yield, the phosphinamide 3a was also isolated in 20% yield (entry 3). In other solvents including methanol, dichloromethane, chloroform, acetone and acetonitrile 4a was obtained in moderate yields (26-35%) along with 3a (10-20%) (entries 4-8). The reaction when carried out in dichloromethane with a 1:2 ratio of 1a and 2a provided 4a in 38% yield, but 3a was also isolated in 30% yield (entry 9). Fortunately, formation of 3a was completely suppressed and 4a could be isolated in 55% yield upon changing the ratio of 1a and 2a to 2:1 (entry 10). Further, a slight reduction in the yield of 4a was noticed upon changing the substrate ratio to 1:3 (entry 11), therefore the conditions in

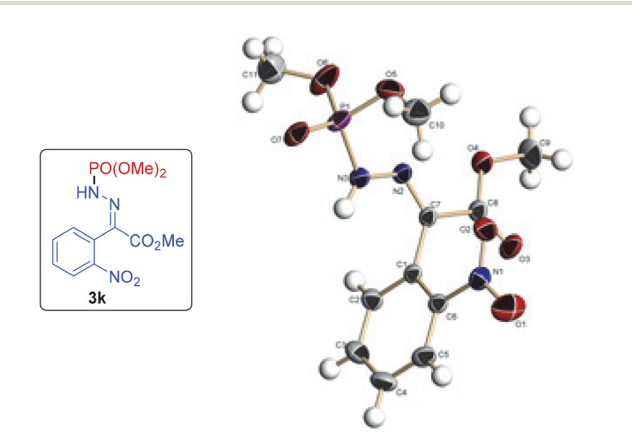


Fig. 1 ORTEP diagram drawn with 30% ellipsoid probability for non-H atoms of the crystal structure of compound 3k determined at 294 K.

Table 3 Optimization of conditions photochemical phosphonylation^{a,b}

	P(OMe) ₃		
N_2	2a	PO(OMe) ₂	_
Ph CO ₂ Me	solvent, rt, N ₂	Ph CO ₂ Me	3a
1a	Blue LEDs (455 nm, 3W)	4a	

Entry	1a:2a	Solvent	Yield of $4a^{c}$ (%)	Yield of $3a^c$ (%)
$\overline{1^d}$	1:1	DMSO	0	0
2^d	1:1	DMF	0	0
3	1:1	PhMe	15	20
4	1:1	MeOH	28	13
5	1:1	CH_2Cl_2	35	10
6	1:1	$CHCl_3$	26	16
7	1:1	$(Me)_2CO$	30	15
8	1:1	MeĆN	30	20
9	1:2	CH_2Cl_2	38	30
10	2:1	CH_2Cl_2	55	<5
11	3:1	CH_2Cl_2	52	<5

a Unless otherwise mentioned, the reactions were carried out on a 0.2 mmol scale of 1a with specified amounts of 2a in 2 mL solvent at rt irradiated with 455 nm blue LEDs under N_2 . b Time taken for reaction completion: 5-6 h. ^c Isolated yields. ^d Complex mixture.

entry 10 were finally selected as the optimal reaction conditions.

Subsequently in order to investigate the scope of the photochemical phosphonylation reaction, several aryl α-diazoeters were employed in the blue light-mediated reaction with trimethylphosphite 2a and triethylphosphite 2b (Table 4). Evidently, phenyl diazo methylesters bearing substituents with various electronic properties performed well under the photoredox conditions to furnish the corresponding C-phosphonylated products 4a-4f in good yields. The diazo substrates with an ethyl ester group and an allyl ester group also reacted efficiently with methylphosphite to afford 4g and 4h in 45% and 66% yield, respectively. The reaction of methyl

Table 4 Scope photochemical phosphonylation diazo compounds^{a,b}

^a Reaction conditions: 1 (0.2 mmol) and 2 (0.1 mmol) in CH₂Cl₂ (2 mL) at rt irradiated with 455 nm blue LEDs under N₂. ^b Isolated yields mentioned. ^c Isolated yield for a 5 mmol scale reaction.

Scheme 2 Plausible mechanism.

2-diazo-2-phenylacetate **1a** with ethylphosphite **2b** under the optimized photoredox conditions furnished **4i** in 60% yield.

Mechanistically, the two phosphonylations follow divergent routes, as depicted in Scheme 2. The N-phosphonylation proceeds through nucleophilic addition of the phosphite to the terminal nitrogen of the diazo group. The resulting zwitterionic intermediate A upon dealkylation during aqueous workup forms intermediate B which tautomerizes to the N-phosphonylated product 3. On the other hand, the aryl diazoester upon visible light-mediated photolysis generates free carbene species X which undergoes insertion with the phosphite to form ylide intermediate Y. Subsequent decomposition of the intermediate Y upon workup leads to the C-phosphonylated product 4. The carbene intermediate in the reaction was confirmed by the formation of dimethyl 2,3-diphenylmaleate, the carbene dimerization product, in the visible light-mediated reaction between 1a and 2a (confirmed by ESMS of crude 4a; Fig. S108 in the ESI†).

Conclusions

In conclusion, we developed mild protocols for accessing phosphonylated hydrazones and phosphonylated aryl carboxylates through thermal and photochemical phosphonylation, respectively, of α -diazocarboxylates with trialkyl phosphites. The former reaction is an example of a nucleophilic substitution reaction whereas the latter reaction follows a carbene insertion pathway. Both reactions proceed under mild reaction conditions, show wide substrate scope and afford the corresponding products in good yields.

Conflicts of interest

There are no conflicts to declare.

Acknowledgements

JP thanks DST, New Delhi for an INSPIRE Ph. D. fellowship. We thank the SAIF division of CSIR-CDRI for the analytical support. We also thank Dr T. S. Thakur of the Biochemistry and Structural Biology Division, CSIR-CDRI for help in X-ray crystal structure determination studies of 3k. CDRI Communication No: 10806.

References

- (a) U. Pradere, E. C. Garnier-Amblard, S. J. Coats,
 F. Amblard and R. F. Schinazi, *Chem. Rev.*, 2014, 114, 9154–9218; (b) S. Demkowicz, J. Rachon, M. Daśko and W. Kozak,
 RSC Adv., 2016, 6, 7101–7112; (c) J. B. Rodriguez and
 C. Gallo-Rodriguez, *ChemMedChem*, 2019, 14, 190–216.
- (a) R. G. Hall, Phosphorus, Sulfur Silicon Relat. Elem., 2008,
 183, 258–265; (b) C. Zhou, X. Luo, N. Chen, L. Zhang and J. Gao, J. Agric. Food Chem., 2020, 68, 3344–3353.
- 3 (a) T. Baumgartner, Acc. Chem. Res., 2014, 47, 1613–1622;
 (b) Z. Wang and T. Baumgartner, Chem. Rec., 2015, 15, 199–217;
 (c) M. A. Shameem and A. Orthaber, Chem. Eur. J., 2016, 22, 10718–10735;
 (d) D. Joly, P.-A. Bouit and M. Hissler, J. Mater. Chem. C, 2016, 4, 3686–3698.
- 4 (a) D. Heift, Z. Benkő and H. Grützmacher, Chem. Eur. J.,
 2014, 20, 11326–11330; (b) C. Xie, A. J. Smaligo, X.-R. Song and O. Kwon, ACS Cent. Sci., 2021, 7, 536–558;
 (c) T. Gensch, G. P. Gomes, P. Friederich, E. Peters, T. Gaudin, R. Pollice, K. Jorner, A. K. Nigam, M. Lindner-D'Addario, M. S. Sigman and A. Aspuru-Guzik, J. Am. Chem. Soc., 2022, 144, 1205–1217.
- 5 (a) Y. Gao, G. Tang and Y. Zhao, Phosphorus, Sulfur Silicon Relat. Elem., 2017, 192, 589–596; (b) K. Neog and P. Gogoi, Org. Biomol. Chem., 2020, 18, 9549–9561; (c) M. Arisawa, Synthesis, 2020, 2795–2806; (d) D. J. Jones, E. M. O'Leary and T. P. O'Sullivan, Adv. Synth. Catal., 2020, 362, 1825–1830; (e) Y. Mei, Z. Yan and L. L. Liu, J. Am. Chem. Soc., 2022, 144(4), 1517–1522; (f) Y. Liu, X. Chen and B. Yu, Chem. Eur. J., 2023, 29, e202302142; (g) X. Liu, L. Zhou, R. Yang, X.-R. Song and Q. Xiao, Adv. Synth. Catal., 2023, 365, 2280–2298.
- 6 For selected reviews on diazo compounds, see: (a) A. Ford, H. Miel, A. Ring, C. N. Slattery, A. R. Maguire and M. A. McKervey, Chem. Rev., 2015, 115, 9981–10080; (b) N. R. Candeias, R. Paterna and P. M. P. Gois, Chem. Rev., 2016, 116, 2937–2981; (c) Y. Xiang, C. Wang, Q. Ding and Y. Peng, Adv. Synth. Catal., 2019, 361, 919–944; (d) Z. Yang, M. L. Stivanin, I. D. Jurberg and R. M. Koenigs, Chem. Soc. Rev., 2020, 49, 6833–6847; (e) P. K. Mykhailiuk, Chem. Rev., 2020, 120, 12718–12755; (f) J. Durka, J. Turkowska and D. Gryko, ACS Sustainable Chem. Eng., 2021, 9, 8895–8918; (g) S. Dong, X. Liu and X. Feng, Acc. Chem. Res., 2022, 55, 415–428; (h) A. Dasgupta, E. Richards and R. L. Melen, ACS Catal., 2022, 12, 442–452; (i) C. Empel, C. Pei and R. M. Koenigs, Chem. Commun., 2022, 58, 2788–2798.
- 7 (a) M. Wang, L. Kong, Q. Wu and X. Li, Org. Lett., 2018, 20(15), 4597–4600; (b) G. G. Faura, T. Nguyen and S. France, J. Org. Chem., 2021, 86, 10088–10104; (c) Z. Qi and S. Wang, Org. Lett., 2021, 23(21), 8549–8553;

- (d) C. Empel, C. Pei, F. He, S. Jana and R. M. Koenigs, Chem. - Eur. J., 2022, 28, e202104397; (e) G. D. Titov, G. I. Antonychev, M. S. Novikov, A. F. Khlebnikov, E. V. Rogacheva, L. A. Kraeva and N. V. Rostovskii, Org. Lett., 2023, 25(15), 2707-2712.
- 8 I. D. Jurberg and H. M. L. Davies, Chem. Sci., 2018, 9, 5112-5118.
- 9 (a) A. M. Polozov, N. A. Polezhaeva, A. H. Mustaphin, A. V. Khotinen and B. A. Arbuzov, Synthesis, 1990, 515-517; (b) W. Miao, Y. Gao, X. Li, Y. Gao, G. Tang and Y. Zhao, Adv. Synth. Catal., 2012, 354, 2659-2664; (c) L. Wu, X. Zhang, Q.-Q. Chen and A.-K. Zhou, Org. Biomol. Chem., 2012, 10, 7859-7862; (d) H. E. Bartrum, D. C. Blakemore, C. J. Moody and C. J. Hayes, Tetrahedron, 2013, 69, 2276-2282;
- (e) L. Wang, Y. Wu, Y. Liu, H. Yang, X. Liu, J. Wang, X. Li and J. Jiang, Org. Lett., 2017, 19, 782-785.
- 10 (a) H. Jiang, H. Jin, A. Abdukader, A. Lin, Y. Cheng and C. Zhu, Org. Biomol. Chem., 2013, 11, 3612-3615; (b) Y. Feng, H. Ding, R. Liu, W. Wei, G. Nan and D. Yi, Asian J. Org. Chem., 2024, 13, e202400015.
- 11 L. B. Balazs, Y. Huang, J. B. Khalikuzzaman, Y. Li, S. A. Pullarkat and P.-K. Leung, J. Org. Chem., 2020, 85, 14763-14771.
- 12 V. K. Aggarwal, J. R. Fulton, C. G. Sheldon and J. de Vicente, J. Am. Chem. Soc., 2003, 125, 6034-6035.
- 13 The crystal structure of compound 3k has been deposited at the Cambridge Crystallographic Data Centre and the reference no. CCDC 2342436 was allotted.†